Spin canting induced nonreciprocal Goos-Hänchen shifts

R. Macêdo,[1,*] **R. L. Stamps,**[1] **and T. Dumelow**[2]

[1]*SUPA, School of Physics and Astronomy, University of Glasgow, Glasgow G12 8QQ, UK*
[2]*Departamento de Física, Universidade do Estado do Rio Grande do Norte, Costa e Silva, 59625-620 Mossoró RN - Brazil*
[*]*RairMacedo@gmail.com*

Abstract: Recent studies on surface reflection illustrate how light beams can be laterally shifted from the position predicted by geometrical optics, the so called Goos-Hänchen effect. In antiferromagnets this shifts can be controlled with an external magnetic field. We show that a configuration in which spins cant in response to applied magnetic fields enhance possibilities of field controlled shifts. Moreover, we show that nonreciprocal displacements are possible, for both oblique and normal incidence, due to inherent nonreciprocity of the polariton phase with respect to the propagation direction. In the absence of an external field, reciprocal displacements occur.

OCIS codes: (040.2235) Far infrared or terahertz; (160.3020) Magneto-optical materials.

References and links

1. R. E. Camley, "Nonreciprocal surface modes," Surf. Sci. Rep. **7**, 103–188 (1987).
2. N. S. Almeida and D. L. Mills "Dynamical response of antiferromagnets in an oblique magnetic field: application to surface magnons," Phys. Rev. B **37**, 3400 (1988).
3. R. L. Stamps, B. L. Johnson, and R. E. Camley "Nonreciprocal reflection from semi-infinite antiferromagnets," Phys. Rev. B **43**, 3626 (1991).
4. K. Abraha and D. R. Tilley, "Theory of far infrared properties of magnetic surfaces, films and superlattices," Surf. Sci. Rep. **24**, 129 (1996).
5. T. Dumelow and R. E. Camley, "Nonreciprocal reflection of infrared radiation from structures with antiferromagnets and dielectrics," Phys. Rev. B **54**, 12232 (1996).
6. T. Dumelow, R. E. Camley, K. Abraha, and D. R. Tilley, "Nonreciprocal phase behavior in reflection of electromagnetic waves from magnetic materials," Phys. Rev. B **58**, 897 (1998).
7. L. Remer, B. Lüthi, H. Sauer, R. Geick, and R. E. Camley, "Nonreciprocal optical reflection of the uniaxial antiferromagnet MnF_2," Phys. Rev. Lett. . **56**, 2752 (1986).
8. D. E. Brown, T. Dumelow, T. J. Parker, K. Abraha, and D. R. Tilley, "Nonreciprocal reflection by magnons in FeF_2: a high resolution study," Phys. Rev. B **49**, 12266 (1994).
9. K. Abraha, D. E. Brown, T. Dumelow, T. J. Parker, and D. R. Tilley, "Oblique incidence far-infrared reflectivity study of the uniaxial antiferromagnet FeF_2," Phys. Rev. B **50**, 6808 (1994).
10. M. R. F. Jensen, T. J. Parker, Kamsul Abraha, and D. R. Tilley "Experimental observation of magnetic surface polaritons in FeF_2 by attenuated total reflection',' Phys. Rev. Lett. **75**, 3756 (1995).
11. T. Dumelow, J. A. P. da Costa, F. Lima, and E. L. Albuquerque. "Nonreciprocal phenomena on reflection of terahertz radiation off antiferromagnets," in *Recent Optical and Photonic Technologies*, Ki Young Kim (Ed.), (InTech, Vukovar, 2010), Chap. 8. http://www.intechopen.com/books/recent-optical-and-photonic-technologies/nonreciprocal-phenomena-on-reflection-of-terahertz-radiation-off-antiferromagnets.
12. F. Lima, T. Dumelow, E. L. Albuquerque, and J. A. P. da Costa, "Nonreciprocity in the Goos–Hänchen shift on oblique incidence reflection off antiferromagnets," J. Opt. Soc. Am. B **28**, 306–313 (2011).
13. F. Goos and H. Hänchen, "Ein neuer und fundamentaler Versuch zur Totalreflexion," Ann. Phys. **436**(7-8), 33–46 (1947).

#222383 - $15.00 USD Received 3 Sep 2014; revised 10 Oct 2014; accepted 10 Oct 2014; published 7 Nov 2014

14. H. K. V. Lotsch, "Beam displacement at total reflection: the Goos-Hänchen effect," Optik **32**, 116,189,299,553 (1970).
15. Miri, A. Naqavi, A. Khavasi, K. Mehrany, S. Khorasani, and B. Rashidian, "Geometrical approach in physical understanding of the Goos-Haenchen shift in one- and two-dimensional periodic structures," Opt. Lett. **33** 2940–2942 (2008).
16. T. Tamir and H. L. Bertoni, "Lateral displacement of optical beams at multilayered and periodic structures," J. Opt. Soc. Am. **61**, 1397–1413 (1971).
17. Y. Huang, B. Zhao, and L. Gao, "Goos-Hänchen shift of the reflected wave through an anisotropic metamaterial containing metal/dielectric nanocomposites," J. Opt. Soc. Am. **29** 1436–1444 (2012)
18. X. -Q Jiang, Z. W Lu, and X. -D Sun, "Control of direction of Goos-Hänchen shift on reflection from a weakly absorbing medium," Optik **122**, 2140–2142 (2011).
19. B. Zhao and L. Gao, "Temperature-dependent Goos-Hänchen shift on the interface of metal/dielectric composites," Opt. Express **17**, 21433–21441 (2009).
20. D. Gao and L. Gao, "Goos-Hänchen shift of the reflection from nonlinear nanocomposites with electric field tunability," Appl. Phys. Lett. **97**, 041903 (2010).
21. W. J. Wild and C. L. Giles, "Goos-Hänchen shifts from absorbing media," Phys. Rev. A **25**, 2099 (1982).
22. P. T Leung, Z.W Chen, and H. -P Chiang, "Large negative Goos-Hänchen shift at metal surfaces," Opt. Commun. **276**, 206–208 (2007) .
23. M. Merano, A. Aiello, G. W 't Hooft, M. P van Exter,E. R Eliel, and J. P Woerdman, "Observation of Goos-Hänchen shifts in metallic reflection," Opt. Express **15**, 15928–15934 (2007).
24. R. Macêdo and T. Dumelow, "Beam shifts on reflection of electromagnetic radiation off anisotropic crystals at optic phonon frequencies," Journal of Optics **15**, 014013 (2013).
25. F. Lima, T. Dumelow, J. A. P. da Costa, and E. L. Albuquerque, "Lateral shift on normal incidence reflection off an antiferromagnet," Europhys. Lett. **83**, 17003 (2008).
26. F. Lima, T. Dumelow, J. A. P. da Costa, and E. L. Albuquerque, "Power flow associated with the Goos-Hänchen shift of a normally incident electromagnetic beam reflected off an antiferromagnet," Phys. Rev. B **79** 155124 (2009).
27. D. L. Mills and E. Burstein, "Polaritons: the electromagnetic modes of media," Rep. Prog. Phys. **37**, 817 (1974).
28. M. McGuirk and C. K. Carniglia, "An angular spectrum approach to the Goos-Hänchen shift," J. Opt. Soc. Am. . **67**, 103–107 (1977).
29. K. Artmann "Berechnung der seitenversetzung des totalrelektierten strahles," Ann. Phys. **437**, 87–102 (1948).
30. T. Dumelow and M. C. Oliveros, "Continuum model of confined magnon polaritons in superlattices of antiferromagnets," Phys. Rev. B **55**, 994 (1997).
31. R. Macêdo and T. Dumelow, "Tunable all-angle negative refraction using antiferromagnets," Phys. Rev. B **89**, 035135 (2014).
32. R. Macêdo R. Rodrigues da Silva, T. Dumelow, and J. A. P. da Costa, "MgF_2 as a material exhibiting all-angle negative refraction and subwavelength imaging due to the phonon response in the far infrared," Opt. Commun. **310** 94–99 (2014).

1. Introduction

Nonreciprocity has been extensively studied for antiferromagnetic structures in the presence of an external field $\mathbf{B}_0$. Effects have been shown theoretically [1–6] and experimentally [7–10], one of the most important being that associated with optical reflection. Nonreciprocity of reflection implies that the properties of the reflected beam for an angle of incidence $+\theta_1$ differ from those for an angle of incidence $-\theta_1$. Affected properties include the intensity [5, 7–9, 11] and phase [6] of the reflected beam, which can change or enhance optical effects.

The nonreciprocal Goos-Hänchen shift on reflection from antiferromagnets is a particularly interesting effect [12]. The Goos-Hänchen effect can be considered as a lateral displacement of a reflected beam at a boundary between two different media. This concept was first investigated experimentally by Goos and Hänchen [13, 14], even though Isaac Newton had predicted such a shift in the reflected beam centuries earlier. There are several studies of such a shift on the external reflection from materials such as photonic crystals [15], multilayered structures [16], metal-dielectric nanocomposites [17], and weakly absorbing media [18]. Tunability of the Goos-Hänchen shift has been explored in terms of temperature [19] and applied electric field [20] dependence in the case of reflection from metal-dielectric composites. In the case of reflection from naturally occurring materials, there exist Goos-Hänchen shifts associated with

#222383 - $15.00 USD Received 3 Sep 2014; revised 10 Oct 2014; accepted 10 Oct 2014; published 7 Nov 2014

the plasma response in metals [21–23] and the far infrared phonon response in crystals such as quartz [24].

In the case of the Goos-Hänchen shift associated with reflection from antiferromagnets, the effect stems from the fact that, at terahertz frequencies, the magnetic component of electromagnetic radiation can interact with the spin precession near magnon-polariton resonances. The resulting shift may become nonreciprocal in the presence of an suitably applied external field $\mathbf{B}_0$. Up to now, studies of Goos-Hänchen shifts in reflection from antiferromagnets have considered only the situation where $\mathbf{B}_0$ is applied along the anisotropy axis, perpendicular to the plane of incidence [12, 25, 26]. In the present work we consider an antiferromagnet in an alternative configuration in which, in the absence of an external field, coupling to the precessing spins only occurs at oblique incidence, leading to narrow reststrahl regions. We consider the resulting Goos-Hänchen shifts in this case, and study the effect of applying an external magnetic field perpendicular to the spin alignment direction, causing the spins to cant. Due to this canting, the resonance frequency is shifted to higher frequencies, and the beam displacement becomes nonreciprocal. Spin canting also leads to displacements at normal incidence.

The paper is organized as follows. Section 2 presents a theoretical background in which the antiferromagnet crystal geometry is presented and reflection from the antiferromagnetic surface is analyzed. Section 3 presents the study of the Goos-Hänchen shifts in the absence of a magnetic field. In Section 4 we consider the effects of an external field $\mathbf{B}_0$ on the reflection from an antiferromagnet at oblique and normal incidence. Conclusions are given in Section 5.

2. Theoretical background

We are interested in the Goos-Hänchen shift for reflection at the boundary between vacuum and a semi-infinite antiferromagnetic crystal as aligned in the coordinate system depicted in Fig. 1. The crystal's easy axis is oriented along x, parallel to the surface, and the incidence plane is xz. We also allow for a static field $\mathbf{B}_0$ applied along the y direction, perpendicular to the anisotropy axis.

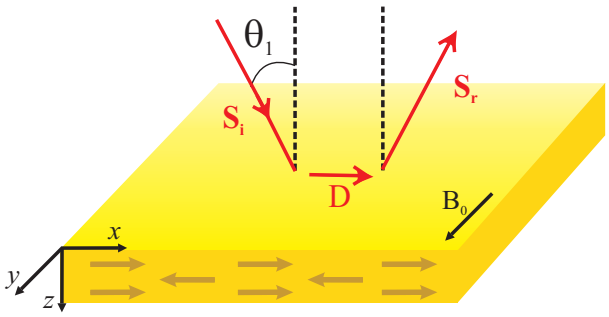

Fig. 1. Schematic representation of an oblique incident beam with an angle θ_1 being displaced on the reflection by a distance D at the interface between vacuum and an antiferromagnet, where S_i and S_r are the incident and reflected Poynting vector respectively.

2.1. *Plane wave reflection from the antiferromagnet*

We consider the situation where a field applied along y cants the spins at an angle α in the plane xy calculated in terms of B_A (magnitude of the anisotropy field) and an exchange field B_E (acting between the spin sublattices). The angle α is then given by

$$\sin\alpha = \frac{B_0}{B_A + 2B_E}. \tag{1}$$

#222383 - $15.00 USD Received 3 Sep 2014; revised 10 Oct 2014; accepted 10 Oct 2014; published 7 Nov 2014

One can show that the antiferromagnetic resonance frequency is [2, 4]

$$\omega_\perp = (\omega_r^2 \cos^2\alpha + 2\gamma^2 B_0 \sin\alpha)^{1/2}. \tag{2}$$

where $\omega_r = \gamma(2B_A B_E + B_A^2)^{1/2}$ and γ is the gyromagnetic ratio. In our geometry the permeability tensor μ takes the form

$$\mu = \begin{pmatrix} \mu_{xx} & 0 & \mu_{xz} \\ 0 & \mu_{yy} & 0 \\ -\mu_{xz} & 0 & \mu_{zz} \end{pmatrix}. \tag{3}$$

We consider only *s*-polarized radiation (**E**-field along *y*, perpendicular to the plane of incidence). In this case, the relevant components are [2]

$$\mu_{xx} = 1 + \frac{2\mu_0\gamma^2 M_S B_0 \sin\alpha}{\omega_\perp^2 - (\omega + i\Gamma)^2}, \tag{4}$$

$$\mu_{zz} = 1 + \frac{2\mu_0\gamma^2 M_S (B_0 \sin\alpha + B_A \cos 2\alpha)}{\omega_\perp^2 - (\omega + i\Gamma)^2}, \tag{5}$$

and

$$\mu_{xz} = -\mu_{xz} = -i\frac{2\mu_0\gamma^2 M_S(\omega + i\Gamma)\sin\alpha}{\omega_\perp^2 - (\omega + i\Gamma)^2}. \tag{6}$$

The complex reflection coefficient r for reflection from an antiferromagnet in the present geometry is

$$r = \frac{k_{z1}(\mu_{xx}\mu_{zz} + \mu_{xz}^2) - k_{z2}\mu_{zz} - k_x\mu_{xz}}{k_{z1}(\mu_{xx}\mu_{zz} + \mu_{xz}^2) + k_{z2}\mu_{zz} + k_x\mu_{xz}}. \tag{7}$$

Here the parallel wavevector component k_x of a plane wave will be given by $k_x = k_0 \sin\theta_1$, where θ_1 is the angle of incidence and $k_0 = \omega/c$. The wavevector components k_{z1} (in vacuum) and k_{z2} (in the antiferromagnet) are given by

$$k_{z1}^2 = k_0^2 - k_x^2 \tag{8}$$

and

$$k_{z2}^2 = \frac{\varepsilon k_0^2(\mu_{xx}\mu_{zz} + \mu_{xz}^2) - k_x^2\mu_{xx}}{\mu_{zz}} \tag{9}$$

respectively, where ε represents the dielectric constant of the antiferromagnet.

2.2. Goos-Hänchen shift on reflection of a finite beam

In the case of reflection of a finite beam, we can still base our analysis on plane wave reflection by considering such a beam as a sum of plane waves. Such a plane wave spectrum approach has been usefully applied to analyzing Goos-Hänchen shifts by McGuirk and Carniglia [28]. Here we summarize the resulting theory for application to the present case.

In this approach, we consider the electric field (directed along *y*) associated with the incident beam as a Fourier sum of plane waves in the form

$$E_i(x,z) = \int_{-k_0}^{k_0} \psi(k_x) e^{i(k_x x + k_{1z} z)}\, dk_x, \tag{10}$$

#222383 - $15.00 USD Received 3 Sep 2014; revised 10 Oct 2014; accepted 10 Oct 2014; published 7 Nov 2014

where k_x is the in-plane component of the wavevector associated with a particular plane wave and $\psi(k_x)$ is a distribution function representing the shape of the beam. The electric field distribution the incident beam at the surface, which we define to be at $z = 0$, ia given by

$$E_i(x,0) = \int_{-k_0}^{+k_0} \psi(k_x) e^{k_x x}\, dk_x, \tag{11}$$

and the electric field distribution of the corresponding reflected beam at the surface is

$$E_r(x,0) = \int_{-k_0}^{+k_0} r(k_x)\psi(k_x) e^{ik_x x}\, dk_x. \tag{12}$$

$r(k_x)$ represents the complex reflection coefficient, which we can represent as

$$r(k_x) = \rho(k_x) e^{i\phi(k_x)}, \tag{13}$$

where $\rho(k_x)$ is the reflection amplitude and $\phi(k_x)$ is the associated phase change on reflection. If this phase change varies with k_x, interference between the reflected plane waves will be different from that for the incident waves, leading to a change in the reflected beam profile. This typically manifests itself as a lateral shift of the reflected beam [26, 28, 29] associated with derivative of $\phi(k_x)$. To see this, consider a wide beam. In this case, k_x assumes a narrow range of values centered around $k_x = k_{x0}$, where $k_{x0} = k_0 \sin\theta_1$, the angle θ_1 being the effective incident angle of the overall beam. If we now expand ρ and ϕ as a Taylor series around $k_x = k_{x0}$, Eq. (12) can be approximated to

$$E_r(x) = r(k_{x0}) \int_{-k_0}^{+k_0} \psi(k_x) exp\left[k_x \left(x + \left.\frac{d\phi}{dk_x}\right|_{k_x = k_{x0}} \right) \right] dk_x, \tag{14}$$

where $r(k_{x0})$ is the reflection coefficient of a plane wave whose angle of incidence is θ_1. The integral representing the profile of the reflected beam in Eq. (14) is the same as that for the incident beam in Eq. (11) except that x has been replaced by $x + D$. Thus the reflected beam has, in effect, been shifted along the surface by a distance D, given by

$$D = -\left.\frac{d\phi}{dk_x}\right|_{k_x = k_{x0}}. \tag{15}$$

3. Zero field Goos-Hänchen shifts

We now apply our theory to reflection of *s*-polarized radiation obliquely incident at a vacuum/MnF_2 interface. MnF_2 is a well characterized antiferromagnet that can be readily prepared and studied experimentally. For this material, the relevant parameters [30] at a temperature of 4.2 K are $M_S = 6.0 \times 10^5$ A/m and $B_A = 0.787$T. The Néel temperature is 67 K and the corresponding exchange field is $B_E = 53.0$ T. Also $\gamma/2\pi c = 0.975$ cm^{-1}/T, corresponding to $\omega_r/2\pi c = 8.94$ cm^{-1}. The damping parameter is $\Gamma/2\pi c = 0.0007$ cm^{-1} and the dielectric constant is $\varepsilon = 5.5$. If $\mathbf{B}_0 = 0$, μ_{zz} has a pole at the resonance frequency 8.94 cm^{-1} and a zero at a somewhat higher frequency close to 9.00 cm^{-1}.

As a first approach we take $\mathbf{B}_0 = 0$. The permeability tensor is then diagonal and r reduces to

$$r = \frac{(\mu_{xx} k_{z1} - k_{z2})}{(\mu_{xx} k_{z1} + k_{z2})}, \tag{16}$$

with

$$k_{z2}^2 = \varepsilon \mu_{xx} k_0^2 - \frac{\mu_{xx}}{\mu_{zz}} k_x^2. \tag{17}$$

#222383 - $15.00 USD Received 3 Sep 2014; revised 10 Oct 2014; accepted 10 Oct 2014; published 7 Nov 2014

In Fig. 2(a) we present the calculated plane wave reflectance $R = rr^*$ spectra, obtained using Eq. (16), for incident angles of $\pm 60^\circ$. Results with and without damping Γ are shown. In each case, there is no difference between the $\theta_1 = +60^\circ$ and the $\theta_1 = -60^\circ$ reflectivity, i.e. the reflectivity is reciprocal $R(\theta_1) = R(-\theta_1)$. This is expected from simple symmetry arguments [1].

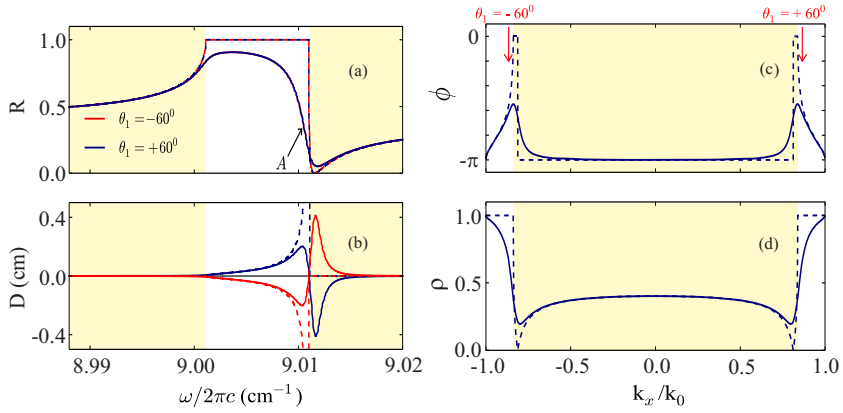

Fig. 2. (a) Calculations of *s*-polarized oblique incidence ($\theta_1 = \pm 60^\circ$) reflection from the interface between vacuum and MnF_2 and (b) Goos-Hänchen shift *D*. Reflected (c) phase and (d) amplitude, as a function of in-plane wavevector k_x, at the frequency marked as *A* in (a) (9.0103 cm^{-1}) for the configuration shown in Fig. 1. Dashed lines are calculated for $\Gamma = 0$, whereas solid lines are for calculations in which $\Gamma = 0.0007$ cm^{-1}. The shaded regions show where transmission is possible in the absence of damping. In case (a) the curves corresponding to $\theta_1 = \pm 60^\circ$ are coincident, so only a blue curve is seen in the case of the solid lines. Note that, in part (c), $\phi = \pi$ is represented as $\phi = -\pi$ in the $\Gamma = 0$ curve for consistency with the $\Gamma = 0.0007$ cm^{-1} curve.

In the case when $\Gamma = 0$, k_{z2} is either wholly real or imaginary. In the case of k_{z2} real, propagation through the antiferromagnet can occur. These regions are indicated by shading in the figures. In the case of k_{z2} imaginary, reflection is total, with no propagation into the antiferromagnet. These are reststrahlen regions. For μ_{xx} positive, the reststrahlen condition is $0 < \mu_{zz} < (1/\varepsilon)\sin^2\theta_1$ which, providing $\theta_1 \neq 0$, is satisfied in a narrow frequency region [31] just above the zero in μ_{zz}. In the configuration considered here, the reststrahlen region only exists at oblique incidence, and its width depends on the angle of incidence. In Fig. 2(a) it is seen that, in the zero damping case (dashed lines), the reflectivity is unity within this region and smaller elsewhere.

In Fig. 2(b) we show the Goos-Hänchen shifts calculated according to Eq. (15). In a similar manner to the result seen for reflectivity, these shifts are found to be reciprocal, which in this case corresponds to the relation $D(+\theta_1) = -D(-\theta_1)$. In the absence of damping, the shifts are nonzero only in the reststrahlen region. This is similar to the behavior of Goos-Hänchen shifts associated with the phonon response in dielectric crystals [32], and can be explained by the fact that in the propagation regions the phase is either 0 or π (i.e. *r* is wholly real) but in the reststrahlen regions it takes on other values.

Since the displacement *D* depends on the derivative of the reflected phase (Eq. (15)), it is useful to plot ϕ and ρ as functions of k_x. In Fig. 2(c) we show $\phi(k_x)$ at the frequency marked as *A* in Fig. 2(a) (9.0103 cm^{-1}), and in Fig. 2(d) we show the corresponding amplitude values ρ, highlighting the values of k_x corresponding to $\theta_1 = \pm 60^\circ$. In the absence of damping, there are important differences between the behavior for $k_x^2/k_0^2 < \varepsilon\mu_{zz}$ (i.e. $\sin^2\theta_1 < \varepsilon\mu_{zz}$) and $k_x^2/k_0^2 >$

#222383 - $15.00 USD Received 3 Sep 2014; revised 10 Oct 2014; accepted 10 Oct 2014; published 7 Nov 2014

$\varepsilon\mu_{zz}$. In the former case, corresponding to propagation regions, the amplitude ρ is less than 1 and the phase ϕ is constant at 0 or π, so that there is no displacement. In the latter case, corresponding to reststrahlen region behavior, the amplitude is unity, corresponding to total reflection, and the phase is continuously varying, leading to nonzero displacement. $\theta_1 = \pm 60^\circ$ corresponds to reststrahlen behavior, resulting in the nonzero shift seen in Fig. 2 at frequency *A*. In the presence of damping, the phase in the bulk region is no longer strictly constant, so a Goos-Hänchen shift is also possible for lower angles of incidence, albeit most markedly in low reflectivity regions.

The lateral displacement of a Gaussian beam obliquely incident on a MnF_2 surface is shown in Fig. 3. In this case the beam is given by Eq. (10) with [26, 31, 32]

$$\psi(k_x) = -\frac{g}{2\cos\theta_1\sqrt{\pi}}\exp\left[-\frac{g^2(k_x-k_{x0})^2}{4\cos^2\theta_1}\right], \tag{18}$$

where $2g$ represents the beam width at the sample surface and θ_1 is the incident angle.

We take $g \approx 2\lambda$, where λ is the free space wavelength of the radiation. The results in Fig. 3 are for the same frequency as that used in Figs. 2(c) and 2(d), i..e Frequency A (9.0103 cm^{-1}). At this frequency the reflectivity is large even when damping is included. We clearly see that the incident beam is positively shifted with a large displacement of around $D = 0.2$ cm (approximately 2λ), in line with the results predicted from Fig. 2(b).

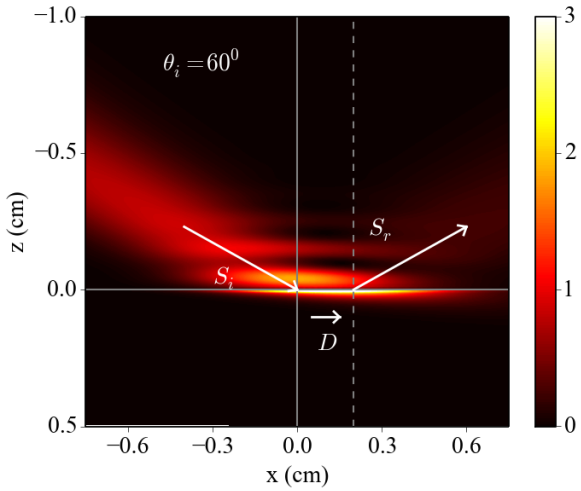

Fig. 3. Calculated overall power intensity (in terms of the magnitude of the time-averaged Poynting vector) showing intensities for a beam of width $g = 0.2$ cm obliquely incident ($\theta_1 = +60^\circ$) on a vacuum/MnF_2 interface at the frequency marked as *A* in Fig. 2 (9.0103 cm^{-1}). The arrows represent the incident and reflected beams, positioned according to Eq. (15), with angle of reflection assumed equal to angle of incidence.

4. Tunable shifts with $\mathbf{B_0 \neq 0}$

Without an external magnetic field the effects associated with external reflection from an antiferromagnetic surface are reciprocal. When a field is applied, nonreciprocal effects, either considered with respect to reversing the sign of the incident angle or that of the applied field, are introduced.

#222383 - $15.00 USD Received 3 Sep 2014; revised 10 Oct 2014; accepted 10 Oct 2014; published 7 Nov 2014

The nonreciprocal behavior considered here is associated with the off-diagonal elements μ_{xz} and μ_{zx} of the permeability tensor. They are nonzero only due to the canting of the spins, which results in a small spin component along the applied field direction.

For the geometry shown in Fig. 1, spin precession is mainly restricted to the yz plane, with the spins on the two sublattices precessing in opposite directions. However, when the spins are canted toward the y axis, one can consider that there is also a small amount of precession in the xz plane. In this plane, the precession direction is the same for both sublattices, but changes direction when the field direction is reversed. The antiferromagnet is thus gyromagnetic, with nonzero permeability components μ_{xz} and μ_{zx} whose signs depend on the field direction. If the incident field of the electromagnetic radiation has a magnetic component in the xz plane, therefore, nonreciprocal effects, such as nonreciprocal Goos-Hänchen shifts, may be expected in reflection.

Nonzero μ_{xz} and μ_{zx} values are also responsible for the nonreciprocal Goos-Hänchen shifts in the previously studied configuration in which the easy axis is taken parallel to the applied field, along y [12, 25, 26]. In such a configuration, however, they become nonzero without the necessity of spin canting. Noticeably higher fields are therefore necessary in the present case than in the previously studied one.

In Fig. 4 we show the effect on the Goos Hänchen shifts of applying an external field. The figure shows how the applied field shifts the resonance to higher frequencies and how the displacement becomes nonreciprocal $D(+\theta_1) \neq -D(-\theta_1)$. The effect of the field on the displacement is distinctly nonlinear, and this appears to be associated with coupling of the incident radiation to surface resonances. In this paper we concentrate on the specific case of $\mathbf{B}_0 = 1.5$ T.

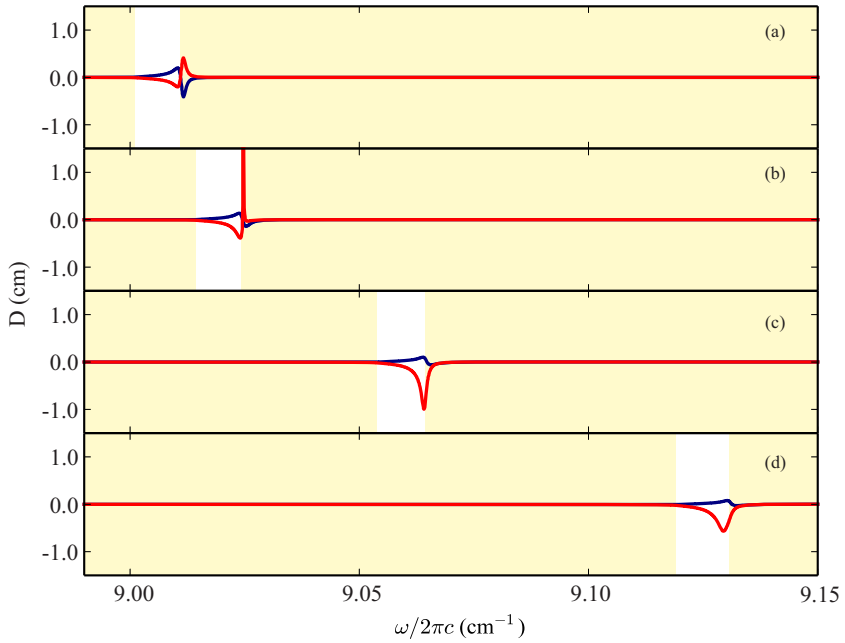

Fig. 4. Goos-Hänchen shift D for different values of applied external field (a) $\mathbf{B}_0 = 0.0$ T, (b) $\mathbf{B}_0 = 0.5$ T, (c) $\mathbf{B}_0 = 1.0$ T and (d) $\mathbf{B}_0 = 1.5$ T. Blue lines are calculated for $\theta_1 = +60^0$, whereas red lines are calculated for $\theta_1 = -60^0$

#222383 - $15.00 USD Received 3 Sep 2014; revised 10 Oct 2014; accepted 10 Oct 2014; published 7 Nov 2014

4.1. *Oblique incidence*

In Fig. 5(a) we show the reflectivity R for oblique incidence ($\theta_1 = \pm 60^0$) reflection from an MnF_2 surface with an external magnetic field $\mathbf{B}_0 = 1.5$ T. All features are now at higher frequencies than in Fig. 2 due to the higher resonance frequency $\omega_\perp$ (Eq. (2)). In the case of $\Gamma = 0$ (dashed lines), both positive and negative angles of incidence give the same result. However, when $\Gamma \neq 0$, $R(+\theta_1)$ and $R(-\theta_1)$ are no longer identical. This is an example of the well-known result that the reflectivity is reciprocal in the absence of damping but can be nonreciprocal when damping is present [1, 3, 7, 8].

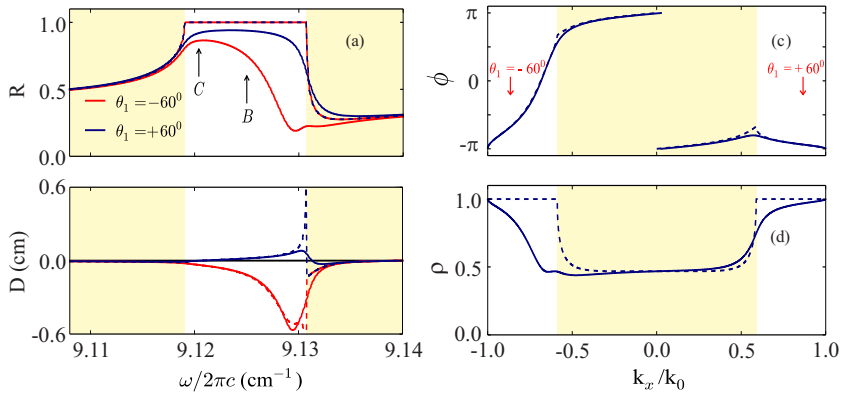

Fig. 5. (a) Calculations of *s*-polarized oblique incidence ($\theta_1 = \pm 60^\circ$) reflection from the interface between vacuum and MnF_2 in the presence of an external magnetic field of 1.5 T and (b) Goos-Hänchen shift D. Reflected (c) phase and (d) amplitude, as a function of in-plane wavevector k_x, at frequency marked as B (9.125 cm^{-1}) in (a). Dashed lines are calculated ignoring damping, whereas solid lines are for calculations in which damping is included. The shaded region shows frequencies where transmission can occur in the absence of damping.

In Fig. 5(b) we show the corresponding Goos-Hänchen shifts. It is immediately seen that the shifts are distinctly nonreciprocal $D(+\theta_1) \neq -D(-\theta_1)$, either with or without damping. Furthermore, there are nonreciprocal shifts some way into the propagation region. Indeed, in the absence of damping, we observe the somewhat counterintuitive property $D(+\theta_1) = D(-\theta_1)$ in this region. Alternatively one could say that, for some given incident angle, reversing the field direction would change the sign of D without changing its amplitude. This result has also been shown for the case of the easy axis perpendicular to the plane of incidence [12].

In Fig. 5(c) we show the reflected phase ϕ as a function of k_x at the frequency marked as B in Fig. 5(a) (9.125 cm^{-1}). In 5(d) we show the corresponding amplitude ρ. The nonreciprocal phase behavior is similar to that discussed by Dumelow *et. al.* [6], and leads to nonreciprocal Goos-Hänchen shifts. For smaller incident angles, corresponding to transmission region behavior ($-0.6 < k_x/k_0 < 0.6$), the amplitude is less than unity in the absence of damping, as in the zero field case. However, the phase is no longer simply 0 or π in this region. It is in fact antisymmetric about $k_x = 0$, so that $\phi(k_x) = -\phi(-k_x)$. This can be shown by resolving Eq. (7) into real and imaginary terms (recalling that μ_{xz} is imaginary in the absence of damping, all other terms being real), and leads to equal derivatives for positive and negative k_x, giving the result discussed above ($D(+\theta_1) = D(-\theta_1)$) for the transmission region frequencies.

For the situation shown in Fig. 5 we are interested in the phase derivative at $\theta_1 = \pm 60^\circ$ (shown as red arrows in Fig. 5(c)). This corresponds to reststrahlen behavior, as anticipated from Fig. 5. $d\phi/dk_x$ is clearly nonzero and its magnitude is different for positive and negative

#222383 - $15.00 USD Received 3 Sep 2014; revised 10 Oct 2014; accepted 10 Oct 2014; published 7 Nov 2014

angles, in agreement with Fig. 5(b), in which nonreciprocity in the Goos-Hänchen shift can be seen. In the absence of damping the amplitude values ρ for positive and negative values of k_x are exactly the same, confirming the results already discussed in relation to Fig. 5(b).

Using the plane wave spectrum model represented by Eqs. (10) and (18), we can simulate a Gaussian beam reflected from an antiferromagnet specimen (as in Fig. 3) in the presence of a nonzero external magnetic field. In the present case we are using the same conditions as in Fig. 5(c). In Fig. 6(a), we show results for a positive incident angle $\theta_1 = +60^\circ$, corresponding to a small displacement of approximately +0.03 cm, as expected from Fig. 5(b). In Fig. 6(b) we show the case for $\theta_1 = -60^\circ$. In this case we can observe a displacement of about -0.1 cm (i.e., $D \simeq -\lambda$), which also agrees with the results shown in Fig. 5(b). Thus, although the sign of the displacement has changed, as expected, the amplitude is considerably larger than in the $\theta_1 = +60^\circ$ case, confirming that the Goos-Hänchen shift is nonreciprocal.

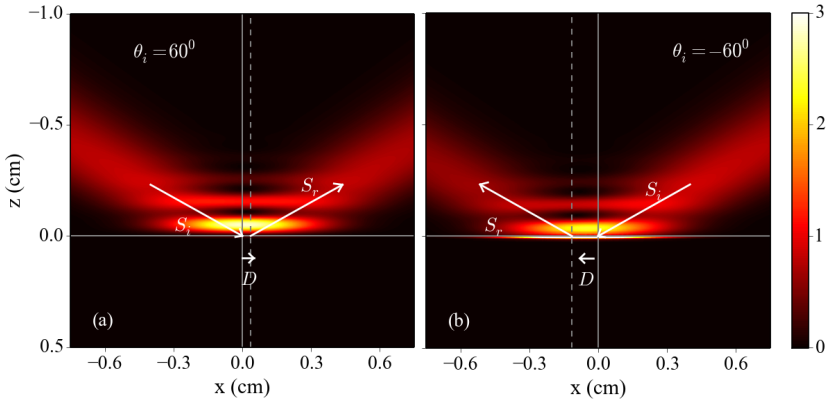

Fig. 6. Calculated overall power intensity (in terms of the magnitude of the time-averaged Poynting vector) showing intensities for a beam of width $g = 0.2$ cm obliquely incident on a vacuum/MnF_2 interface at frequency B ($\omega = 9.125$ cm^{-1}) in the presence of a magnetic field $B_0 = 1.5$ T. (a) $\theta_1 = +60^\circ$; (b) $\theta_1 = -60^\circ$ .The arrows represent the incident and reflected beams, positioned according to Eq. (15), with angle of reflection assumed equal to angle of incidence.

4.2. Normal incidence

We now consider the possibility of a normal incidence Goos-Hänchen shift of the type discussed by Lima *et. al.* [25,26] for the case of the antiferromagnet easy axis parallel to the applied field. In the absence of an external field, the reflected phase is reciprocal [i.e., $\phi(+k_x) = \phi(-k_x)$], so $d\phi/dk_x$ will be zero at normal incidence ($k_x = 0$), resulting in a zero shift. In fact, as discussed in Section II, there is no reststrahlen region associated with normally incident radiation, and no magnon-polariton related phenomena are expected. In the presence of a nonzero external field, however, due to the more complex nature of the permeability tensor represented by Eq. (3), a narrow reststrahlen region does appear at normal incidence. This can be seen from Fig. 7(a), which shows the normal incidence reflectivity in the presence of a an applied field of 1.5 T, i.e., the same configuration as in the Fig. 5 but at normal incidence. We can see that there is a narrow reststrahlen region, centered around 9.12 cm^{-1}. In this region, the reflectivity is unity in the absence of damping, although it is considerably less in the presence of damping.

Figure 7(b) shows the normal incidence Goos-Hänchen shift, which is nonzero both inside and outside the reststrahl region. At frequency B, in the bulk region, there is small negative

#222383 - $15.00 USD Received 3 Sep 2014; revised 10 Oct 2014; accepted 10 Oct 2014; published 7 Nov 2014

shift, as predicted from Fig. 5(c). At frequency C (9.1204 cm^{-1}), within the reststrahlen region, however, a considerably larger displacement of about -0.05 cm is observed with a reasonable reflectivity.

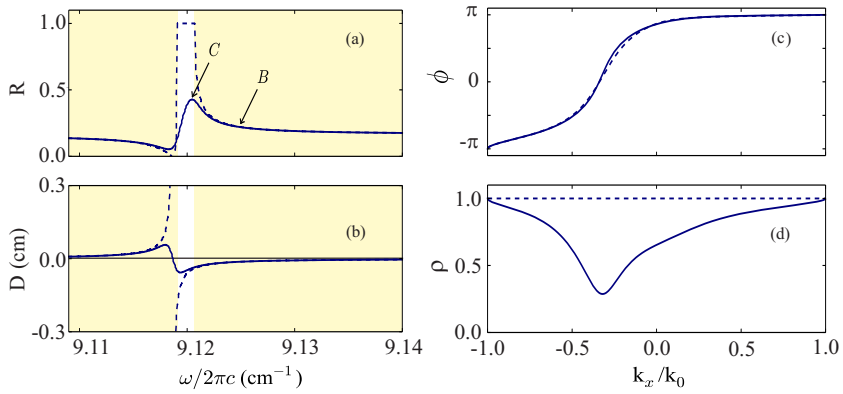

Fig. 7. Normal incidence calculations in the presence of an external magnetic field of 1.5 T. (a) Plane wave reflectivity spectrum; (b) Goos-Hänchen shift D. Reflected (a) phase and (b) amplitude, as a function of in-plane wavevector k_x, for s-polarized reflection from a MnF_2 crystal at the frequency marked in C as (a) (9.1204 cm^{-1}), in the presence of an external magnetic field of 1.5 T. Dashed lines are calculated ignoring damping, whereas solid lines are for calculations in which damping is included. The shaded regions show where transmission can occur in the absence of damping.

The reflected phase ϕ (Fig. 7(c)) and the amplitude ρ (Fig. 7(d)) are shown, as a function of k_x, for frequency C. The dashed lines show results without damping and the solid lines show results with damping included. At this frequency, reststrahlen behavior is present for all incident angles, so the amplitude is always unity, ignoring damping. It is seen that $\phi(k_x)$ is nonreciprocal and has nonzero derivative when k_x is zero, with or without damping. This results in a significant nonzero Goos-Hänchen shift consistent with Fig. 7(b).

The lateral displacement at frequency C (see Fig. 7(a)) can be seen in Fig. 8 where we show the beam intensity profile (i.e. $|E|^2$) of a normally incident beam. For this simulation we use the model described by Eqs. (10) and (18). However, when θ_1 is equal to zero, the function ψ reduces to

$$\psi(k_x) = -\frac{g}{2\sqrt{\pi}} \exp\left(-\frac{g^2 k_x^2}{4}\right). \tag{19}$$

For a normal incidence we increase the width of the beam to $g \approx 5\lambda$ in order to better simulate the wide beam approximation inherent in Eq. (14). We can see clearly from the resulting profile in Fig. 8 that there is a shift of the reflected beam at the sample surface in accurate agreement with the result shown in Fig. 7, based on Eq. (15). The vertical solid line represents the center of the incident beam at $x = 0$, and the vertical dashed line represents the center of the reflected beam, which is slightly dislocated to the left ($x = -0.04$ cm).

In addition to using Fig. 7(c) in interpreting normal incidence results, we make some additional observations with regard to its use in interpreting Goos-Hänchen shifts at oblique incidence at frequency C. Firstly, at this frequency, it is seen that $d\phi/dk_x$ is always positive regardless of the sign of k_x, so the sign of the shift should always be negative regardless of the sign of the incident angle (alternatively, reversing the sign of the applied field would always change the sign of the shift). We can see this using the example of $\theta_1 = \pm 60^\circ$, already considered in the previous section. Figure 5(b) confirms that the expected behavior does indeed occur

#222383 - $15.00 USD Received 3 Sep 2014; revised 10 Oct 2014; accepted 10 Oct 2014; published 7 Nov 2014

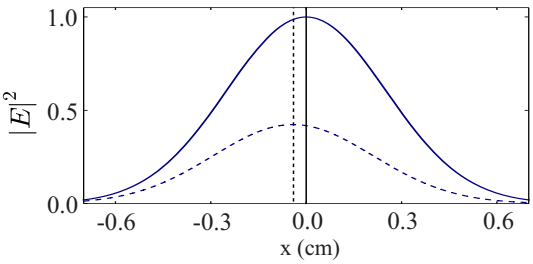

Fig. 8. Intensity profiles of the incident (solid curve) and reflected (dashed curve) gaussian beam of width $g = 0.5$ cm, at the frequency marked as *C* as Fig. 7 (9.1204 cm^{-1}), normally incident on MnF_2 in the presence of a magnetic field B_0 = 1.5 T, with damping effects taken into account. The vertical solid line represents the center of the incident beam ($x = 0$) and the vertical dashed line represents the center of the reflected beam ($x = -0.04$ cm).

at frequency *C*. For $\theta_1 = +60^\circ$, there is a very small negative displacement, reflecting the fact that the derivative of $\phi(k_x)$ is small and positive. For $\theta_1 = -60^\circ$, there is a somewhat larger negative displacement, as predicted from the derivative of the $\phi(k_x)$ curve in Fig.7(a).

A second observation with regard to this figure concerns a comparison of the phase behavior in Fig. 7(c) with the amplitude behavior in Fig. 7(d). As can be seen, the amplitude turns out to be extremely nonreciprocal when damping effects are included. In fact it reaches a minimum within the negative k_x regime where the phase has a large derivative, i.e. where the shift *D* will be large. When this occurs, both k_x and *D* are negative, i.e., they are both in the same direction, resulting in what would normally be described as a positive Goos-Hänchen shift. This implies an increased penetration into the antiferromagnet, so it is reasonable to expect a higher absorption. In the case of a negative Goos-Hänchen shift (positive k_x) there is less penetration, and hence less absorption [12].

5. Conclusions

We have considered the reflection of terahertz radiation from an uniaxial antiferromagnetic crystal (MnF_2) with its uniaxis in the plane of incidence, parallel to the antiferromagnet surface. We find that large Goos-Hänchen shifts ($D \approx 0.2$ cm) for external reflections from an antiferromagnetic crystal are possible. Using an *s*-polarized terahertz beam, we show that, in the absence of an external magnetic field, these shifts are reciprocal ($D(+\theta_1) = -D(-\theta_1)$) and only occur in the reststrahlen regions. These reststrahlen regions only exist at oblique incidence and are much narrower than when the spins are perpendicular to the plane of incidence (the case studied by Lima *et. al.* [12]).

We have shown that a magnetic field B_0 externally applied perpendicular to the uniaxis can induce nonreciprocity. This nonreciprocity is associated with a spin component parallel to the applied field. This particular spin component only exists due to canting of the spins, and for this effect to be evident somewhat higher fields than in the previously studied case, in which the uniaxis is parallel to the field, are necessary. The magnitude of non-reciprocal effects is largely associated with coupling of the incident radiation to surface resonances, and this aspect deserves further study.

Acknowledgments

The authors have benefited from useful discussions with Scott G. Smith. This work was supported by the Engineering and Physical Sciences Research Council (EPSRC grant number EP./L002922/1), the Brazilian Agency CNPq and the University of Glasgow.

#222383 - $15.00 USD Received 3 Sep 2014; revised 10 Oct 2014; accepted 10 Oct 2014; published 7 Nov 2014